

1 Classification: Biological Sciences

2

3

4

5 **Telomere shortening produces an inflammatory environment that**  
6 **promotes tumor invasiveness in zebrafish**

7

8 Kirsten Lex<sup>1\*</sup>, Mariana Maia Gil<sup>1\*</sup>, Margarida Figueira<sup>1</sup>, Marta Marzullo<sup>1</sup>, Bruno Lopes-

9 Bastos<sup>1,3</sup>, Kety Giannetti<sup>1</sup>, Tania Carvalho<sup>2</sup> and Miguel Godinho Ferreira<sup>1,3</sup>

10

11 <sup>1</sup> Instituto Gulbenkian de Ciência, 2781-901 Oeiras, Portugal

12 <sup>2</sup> Histology and Comparative Pathology Laboratory, Instituto de Medicina Molecular, 1649-  
13 028 Lisbon, Portugal

14 <sup>3</sup> Institute for Research on Cancer and Aging of Nice (IRCAN), INSERM U1081 UMR7284  
15 CNRS, 06107 Nice, France.

16

17 \* These authors contribute equally in this work

18

19

20

21

22

23

24 Corresponding Author: [Miguel-Godinho.FERREIRA@unice.fr](mailto:Miguel-Godinho.FERREIRA@unice.fr)

25

26 Keywords: Telomeres, Telomerase, Cancer, Inflammation, Aging

27

28 **Abstract**

29       Cancer incidence increases exponentially with age, when human telomeres are  
30       shorter. Similarly, telomerase mutant zebrafish (*tert*) have premature short telomeres and  
31       anticipate cancer incidence to younger ages. However, because short telomeres constitute a  
32       road block to cell proliferation, telomere shortening is currently viewed as a tumor suppressor  
33       mechanism and should protect from cancer. This conundrum is not fully understood. In our  
34       current study, we report that telomere shortening promotes cancer in a non-cell autonomous  
35       manner. Using zebrafish chimeras, we show increased incidence of invasive melanoma when  
36       WT tumors are generated in *tert* mutant zebrafish. *tert* zebrafish show increased levels of  
37       senescence (*cdkn2a* and *ink4a/b*) and inflammation (*TNF- $\alpha$* ). In addition, we transferred  
38       second generation *tert* blastula cells into WT to produce embryo chimeras. Cells with very  
39       short telomeres induced senescence and increased neutrophil numbers in surrounding larval  
40       tissues in a non-cell autonomous manner, creating an inflammatory environment. Considering  
41       that inflammation is pro-tumorigenic, we transplanted melanoma-derived cells into second  
42       generation *tert* zebrafish embryos and observed that tissue environment with short telomeres  
43       leads to increased micrometastasis. To test if inflammation was necessary for this effect, we  
44       treated melanoma transplants with non-steroid anti-inflammatory drugs and show that higher  
45       melanoma invasiveness can be averted. Thus, apart from the cell autonomous role of short  
46       telomeres in contributing to genome instability, we propose that telomere shortening with age  
47       causes systemic chronic inflammation leading to increased tumor incidence.

48

49

## 50      **Significance Statement**

51      Cancer incidence increases exponentially in human midlife. Even though mutation  
52      accumulation in somatic tissues results in increased tumorigenesis, it is currently not  
53      understood how aging contributes to cancer. Telomeres, the ends of eukaryotic linear  
54      chromosomes, shorten with each cell division. Here we show that telomere shortening  
55      contributes to cancer in a non-cell autonomous manner. Using embryo chimeras of  
56      telomerase deficient zebrafish generated from melanoma-prone fish, we show that tumors  
57      arise more frequently and become more invasive in animals with shorter telomeres. Telomere  
58      shortening gives rise to increased senescence and systemic inflammation. We observed  
59      increased melanoma metastasis dissemination in zebrafish larvae with very short telomeres.  
60      Thus, telomere shortening similar to human aging, generates a chronic inflammatory  
61      environment that increases cancer incidence.

62

## 63      **Introduction**

64              Cancer incidence increases exponentially in the mid-decades of human life (1).  
65              Although mutations are required to build-up during tumorigenesis, the overall post-  
66              reproductive incidence opens the possibility of organism-based causes for the increase of  
67              cancer with age. Due to absence of telomerase expression in most somatic tissues, telomeres  
68              shorten as we grow older (2). Telomeres constitute the ends of eukaryotic chromosomes and  
69              are constituted by repetitive DNA sequences (TTAGGG)<sub>n</sub> recognized by a protein complex  
70              called shelterin (3). This structure prevents chromosome-ends from being recognized as  
71              deleterious DNA double strand breaks while counteracting their slow attrition, resulting from  
72              the “end-replication problem” by recruiting telomerase. Humans are born with telomeres  
73              between 10-15 kb long (4) and, due to continuous cell divisions, telomeres may reach a  
74              critical length. As cell division reaches the Hayflick limit, telomeres are recognized as DNA  
75              damage and block cell proliferation either by undergoing senescence or apoptosis (5-7).  
76              Since short telomeres block cell division, telomere shortening is considered as a tumor  
77              suppressor mechanism by preventing excessive cell proliferation. Indeed, telomerase is  
78              frequently re-activated in the majority of cancer cells, allowing for cell immortalization  
79              thereby escaping replicative senescence. In line with this idea, anti-telomerase therapies are  
80              currently undergoing clinical trials for cancer therapy (8).

81              Countering the tumor suppressor hypothesis, telomere shortening may lead to genome  
82              instability, a hallmark of cancer. Because loss of telomere protection results in breakage-  
83              fusion-bridge cycles, the ensuing genome instability may contribute for age-dependent  
84              tumorigenesis (9). An extreme example of the pro-tumorigenic effect of short telomeres  
85              occurs in “telomeropathies”. People carrying mutations in telomerase or related proteins have  
86              pathologically short telomeres in early life (10, 11). Despite exhibiting pathologies related to  
87              deficiencies in cell proliferation, patients also suffer from an increased cancer risk (12).

88 Similarly, our work on the telomerase mutant zebrafish, which undergoes premature telomere  
89 shortening, revealed that they anticipate cancer incidence to early life (13). Even though short  
90 telomeres positively correlate with increased tumorigenesis in both humans and zebrafish, it  
91 is not yet understood how telomere shortening may lead to cancer.

92 Telomere shortening has consequences beyond the cellular level. As cells approach  
93 replicative senescence, DNA damage emanating by short telomeres initiate a cascade of  
94 events that expands to the extracellular environment. Senescent cells were shown to release a  
95 set of molecules termed senescence-associated secretory phenotype (SASP) (14). SASP was  
96 described *in vitro* and is mainly constituted by chemokines, growth factors, extra cellular  
97 matrix remodelers and other inflammatory factors, capable of modulating cell environment.  
98 These molecules were posteriorly shown to influence the ability of other cells to divide,  
99 potentially having a pro-tumorigenic effect (15). Consistently, repeated wounding in  
100 zebrafish stimulates inflammatory responses, which were shown to promote cancer  
101 progression (16, 17). Therefore, we hypothesize that telomere shortening contribution to  
102 tumorigenesis may have a non-cell autonomous component. In aging organisms, cells  
103 undergoing replicative senescence would comprise a source of SASP/inflammatory factors  
104 creating a pro-tumorigenic environment. In agreement with our hypothesis, population  
105 studies have associated the long-term use of anti-inflammatory agents (acetylsalicylic acid)  
106 and a reduction risk of several cancers (18–20).

107 Here we show that tissues containing cells with short telomeres promote increased  
108 cancer incidence in a non-cell autonomous manner. Using chimeric zebrafish, we observed  
109 that telomerase-proficient melanocytes expressing HRAS give rise to more melanoma tumors  
110 when surrounded by *tert* mutant cells. Melanomas developed in this environment exhibited  
111 high invasiveness as observed by histopathology. In agreement, using zebrafish tumor  
112 transplants, we show that HRAS melanoma cells expand faster when injected into second-

113 generation (G2) *tert* mutant larvae. Both adult G1 *tert* and G2 *tert* larvae have higher levels  
114 of senescence and SASP/inflammation. G2 *tert* cells injected into WT embryos stimulate  
115 senescence and inflammation in a non-cell autonomous manner. Chemical inhibition of  
116 inflammation in G2 *tert* embryos rescued the invasiveness capacity of melanoma cells. Thus,  
117 cells with short telomeres are capable of inducing senescence and inflammation, creating a  
118 pro-tumorigenic environment that results in higher cancer invasiveness.

119

120 **Results**

121 ***tert* mutant environment causes higher tumor incidence in a non-cell autonomous  
122 manner**

123 Similar to mammals, zebrafish tumor microenvironment (TME) modulates cancer  
124 behavior (21, 22). Tumors may be inhibited or enhanced as a consequence of the dynamic  
125 crosstalk between cancer and surrounding cells. We, therefore, asked what were the effects of  
126 a TME with short telomeres on emergent tumors.

127 In order to study the non-cell autonomous effects of TME telomere shortening in  
128 cancer, we wanted to separate telomerase expression of pre-cancer cells from their  
129 surrounding tissues and, for this purpose, we generated chimeric zebrafish using early-  
130 developmental embryo transplants. We used a melanoma zebrafish model (*mitfa*:HRAS)  
131 developed by the Hurlstone lab that exhibits full penetrance by 3 months of age (23). We  
132 chose this model since it did not require an initial *tp53* dysfunction to form tumors and we  
133 had previously shown that loss of p53 function rescues *tert* zebrafish mutants (24). Blastula  
134 cells from donor embryos capable of giving rise to melanoma were transplanted into WT or  
135 *tert*-/- recipients (Fig 1A). In addition, recipient embryos had a *casper* genetic background  
136 (*mitfa*<sup>w2/w2</sup>; *mpv17*<sup>a9/a9</sup>), and lacked the ability to produce melanocytes. Consequently, all

137 melanoma could only arise from donor cells. Embryo chimeras then were allowed to grow  
138 into adulthood and studied for tumor incidence. As expected, we observed the development  
139 of melanoma lesions, typically in the anal fin region of both WT and *tert*-/- recipient fish  
140 (Fig. 1B). However, by 30 weeks, a time when *tert*-/- associated lethality is still low (<20%),  
141 20% of WT chimeras developed tumors, while ca. 50% of *tert*-/- chimeras exhibited  
142 melanoma (Fig. 1C, p<0.05). Thus, we found that *tert*-/- recipients significantly increased  
143 tumor incidence by ca. 2-fold (Hazard ratio after Mantel-Haenszel calculation: 2.0 when  
144 compared with WT fish).

145 A possible explanation for the observed differences of tumor development in a WT  
146 vs. *tert*-/- environment is cell competition. Wildtype tumor-prone cells could be fitter and  
147 more efficient in outcompeting *tert* mutant recipient cells, possibly due to higher proliferation  
148 rates. Thus, fitter donor cells could produce higher number of melanocytes expressing HRAS  
149 in *tert* mutant recipients and, subsequently, lead to a higher tumor incidence. To test this  
150 hypothesis, we quantified the number of melanocytes at two stages of embryo development at  
151 3- and 11-days post-fertilization (dpf) in both *tert* mutant and WT recipients. Contrary to our  
152 hypothesis, we observed no significant increase in the number of melanocytes in *tert*-/-  
153 recipients as compared to WT during developmental stages (Supplementary Figure 1A-B). In  
154 case growth differences would only be visible at later stages, we quantified the surface area  
155 covered by the melanocytic lesions in adult animals. Percentage of pigmentation was  
156 quantified for WT and *tert*-/- zebrafish (Supplementary Figure 1C-D). Similar to the results  
157 obtained in larvae, although there was variation between individuals, we did not observe  
158 significant differences when comparing host genotypes. Together, our data indicates that a  
159 *tert* mutant TME increases tumor incidence in a non-cell autonomous manner, suggesting that  
160 telomere shortening has a systemic role in cancer beyond the one described in genome  
161 stability.

162

163 **Tumors progress faster in *tert* mutant TME**

164 Among the hallmarks of cancer, one qualitative difference between cancers relies on  
165 the capacity to invade different tissues. Zebrafish chimeras bearing melanoma were analyzed  
166 by histopathology and ranked according to their staging and invasiveness. Overall, 84% of  
167 samples (N=43) that were macroscopically defined as tumors were confirmed as malignant  
168 tumors in histopathological analysis (Fig. 2 A-C). The remaining samples were staged as  
169 benign tumors or melanosis. The large majority of tumors in *tert*-/- recipients were invasive  
170 (80%, N=10; Fig. 2 B). In comparison, only 22% of tumors exposed to a wildtype  
171 environment (N=9) were determined as invasive (Fig. 2 B). A similar result was found when  
172 malignant tumors were scored for the presence of cellular atypia. Cellular atypia describes  
173 cytologic structural abnormalities and is a marker for more transformed cancers and more  
174 advanced staging (25). Whereas 71% of tumors in a *tert*-/- environment (N=7) exhibited  
175 moderate levels of cellular atypia (Fig. 2 C), all tumors in WT recipients showed low levels  
176 (N=5). These results indicate that melanoma developed in *tert*-/- recipients progress faster,  
177 reaching advanced stages faster and becoming more invasive, suggesting that TME telomere  
178 shortening not only increase tumor incidence but its progression.

179

180 **Zebrafish melanoma transplants are more invasive in *tert* mutant larvae**

181 We and others have shown that injection of tumor cells in zebrafish larvae constitutes  
182 an assay to study invasiveness capacity of cancer cells (26, 27). This constitutes a simpler  
183 assay and allows for more expedite manipulations while being amenable to chemical studies.

184 In order to confirm that *tert*-/- TME promotes tumor invasiveness, we injected  
185 melanoma cells derived from HRAS tumors into 2dpf WT and *tert*-/- larvae (Fig. 3A). To  
186 ensure that these fish would possess cells with critically short telomeres, we used second

187 generation *tert*-/ (G2 *tert*-/) resulting from an in-cross of young adult *tert*-/ zebrafish. In  
188 contrast to G1 *tert*-/ derived from heterozygous parents, G2 *tert*-/ embryos possess very  
189 short telomeres and a high mortality with an average longevity of ~12days (28, 29). We  
190 dissected melanomas from HRAS tumors expressing GFP (see Methods) and injected cells  
191 into the blood circulation of 2dpf larvae. Injected melanoma cells preferentially accumulate  
192 in the tail region from where, depending on their invasiveness capacity, disseminate to  
193 neighboring tissues (Fig. 3B). Injected larvae were individually followed over time and the  
194 area occupied by GFP cells was quantified (Fig. 3B).

195 If an environment with short telomeres promotes tumor invasiveness, then injected  
196 melanoma cells should disseminate more when injected in G2 *tert*-/ when compared to WT  
197 larvae. We quantified the GFP-area at 1, 4 and 7 days-post injection (Fig. 3C). We calculated  
198 the linear regression between the 3 time-points and obtained a progression slope for the  
199 expansion of each grafted melanoma (N=31). We observed that *tert*-/ recipients allowed for  
200 a more accentuated progression than the WT ones (Fig. 3D). Thus, our results using tumor  
201 transplants indicate that melanoma cells disseminate faster in G2 *tert*-/ than WT larvae,  
202 suggesting that telomere shortening in aging individuals could promote tumor progression in  
203 a non-cell autonomous manner.

204  
205 **G2 *tert*-/ cells are senescent and inflammatory and capable of modulating their  
206 surrounding environment.**

207 Telomere shortening is responsible for replicative cell senescence in human cultured cells  
208 (30). Accordingly, we expected that *tert*-/ zebrafish would present increased levels of  
209 senescence. Using RT-qPCR for specific genes, we quantified the levels of senescence in  
210 *tert*-/ 9month-old adult tissue (intestine) and 4dpf G2 *tert*-/ larvae (whole). As expected, the  
211 senescence markers *ink4a/b* (p15/16) and *cdkn1a* (p21) levels were significantly higher in

212 both G1 *tert*−/− adults and G2 *tert*−/− larvae than in WT controls (Fig. 4A-B). In addition,  
213 using the SA-β-Gal assay, we confirmed higher levels of senescence localized primarily in  
214 the head and notochord of G2 *tert*−/− larvae (Fig. 4D).

215 Senescent cells were shown to secrete a set of molecules, known as SASP, mainly  
216 composed of inflammatory factors (14, 15). Therefore, we asked if *tert*−/− zebrafish present  
217 signs of inflammation. We measured expression levels of TNF-α, one of the main cytokines  
218 expressed during an inflammatory response, by RT-qPCR. Indeed, both G1 *tert*−/− adults and  
219 G2 *tert*−/− larvae showed elevated levels of TNF-α when compared to WT (Fig. 4C).  
220 Interestingly, undisturbed 9month-old WT zebrafish exhibit higher levels of TNF-α than  
221 4day-old larvae, suggesting that aging animals may respond similarly to young *tert*−/−  
222 mutants. Together, our results suggest that telomere shortening in zebrafish results in  
223 increased senescence and inflammation.

224 Given the nature of the responses, we wondered if these observations originated from  
225 cell-autonomous effects of *tert*−/− cells dispersed through the body or if *tert*−/− cells could  
226 modulate their extracellular environment *in vivo* and generate a systemic response. To test if  
227 short telomere *tert*−/− cells modulate their extracellular environment, we transplanted GFP-  
228 labelled G2 *tert*−/− cells during early-development into WT recipient embryos, thereby  
229 generating larvae chimeras (Fig. 4E). Even though we transferred few G2 *tert*−/− cells into  
230 developing embryos (<1% as measured by FACS of desegregated embryos at 4dpf), they  
231 were sufficient to increase overall SA-β-Gal levels (Fig. 4E). Interestingly, we observed a  
232 similar pattern of SA-β-Gal staining in these chimeras as in G2 *tert*−/− larvae (N=22) at the  
233 same stage of 4dpf (compare Fig. 4D with 4E). These results suggest that cells derived from  
234 G2 *tert*−/− embryos are capable of inducing senescence in a non-cell autonomous manner, thus  
235 constituting an example of paracrine SASP.

236 Since senescent cells secrete pro-inflammatory molecules, we asked if G2 *tert*−/− cells

237 with short telomeres could create an inflammatory environment in newly generated chimeras.  
238 To test this, we generated similar embryo chimeras in Tg(*mpx:GFP*) recipient zebrafish that  
239 carry GFP-labelled neutrophils (31). As before, we injected both WT and G2 *tert*−/− cells  
240 from embryos at blastula stage into Tg(*mpx:GFP*) recipient embryos of the same stage and  
241 observed its effects in 4dpf larvae (Fig. 4F, right). Whereas WT cells generated zebrafish  
242 larvae (N=33) with similar numbers of neutrophils as un-injected embryos, Tg(*mpx:GFP*)  
243 chimeras carrying G2 *tert*−/− cells (N=25) exhibited higher numbers of neutrophils (Fig. 4F,  
244 p=0.0075). Thus, since these innate immune cells are key to inflammatory responses, G2 *tert*−/−  
245 cells give rise to a systemic inflammatory environment. Together, our results indicate that  
246 telomerase deficient zebrafish undergo senescence and produce an inflammatory state.  
247 Moreover, we show that this effect is non-cell autonomous with *tert*−/− cells impacting the  
248 surrounding tissues modulating their environment, creating a senescent and inflammatory  
249 environment.

250

251 **Chemical inhibition of inflammation rescues melanoma dissemination in the G2 *tert*−/−  
252 mutant larvae.**

253 Inflammation can induce transformed cell growth (32). In zebrafish, PGE<sub>2</sub> produced  
254 by innate immune cells via the COX-2 pathway was shown to act as key growth factor at the  
255 earliest stages of tumor progression (16, 33). We hypothesized that the inflammatory  
256 environment induced by *tert*−/− cells could underlie the enhanced melanoma invasiveness  
257 observed in *tert* mutant zebrafish. To test this hypothesis, we treated the previously generated  
258 zebrafish melanoma larvae allografts with non-steroid anti-inflammatory drugs (NSAIDs):  
259 Aspirin (COX-1 and 2 inhibitor) and Celecoxib (COX-2 specific inhibitor). As previously,  
260 we measured melanoma invasiveness by quantifying the GFP area at consecutive timepoints  
261 upon melanoma cell injections (1, 4 and 7 dpi). Both WT and G2 *tert*−/− recipients were kept

262 in embryo medium containing Aspirin (30 $\mu$ M) or Celecoxib (25 $\mu$ M) for the duration of the  
263 experiment. As previously, we calculated a progression slope of tumor cells per transplanted  
264 zebrafish and compared treated vs. untreated larvae (Fig. 5A-B). As previously, control  
265 groups showed an increased invasiveness of melanoma cells when transplanted into G2 *tert*-/-  
266 (N=31) than in WT larvae (N=32) (Fig. 5D, p= 0.0205). However, upon NSAID treatment,  
267 the increased invasion capacity of HRAS cells in G2 *tert*-/- larvae (N=20) decreased to WT  
268 levels (N=19) (Fig. 5C-D, Aspirin p=0.7897; Celecoxib: p= 0.1605). Together, our result  
269 suggests that the inflammatory environment induced by *tert*-/- cells promotes melanoma  
270 invasiveness via the COX-2 pathway. We showed an increase of innate immune cells in  
271 larvae containing telomerase deficient cells (Fig. 4F). Thus, in agreement with previous  
272 studies (16, 33, 34), we propose that neutrophils, by producing larger amounts of  
273 prostaglandins, may enhance melanoma invasiveness.

274

275 **Discussion**

276 Studies on how telomerase affects tumorigenesis have focused primarily on the cell-  
277 autonomous role of telomere shortening in cancer cells (9). Indeed, telomerase is reactivated  
278 in the majority of cancer cells promoting cancer development. Consistently, telomerase  
279 promoter mutations that result in increased telomerase expression are now recognized as one  
280 of the most common alterations in cancer (35). However, cancer incidence increases  
281 exponentially in the mid-ages of human life, a time when telomeres are shorter (1, 2). In our  
282 current study, we attempted to understand why cancer incidence increases when telomeres  
283 are shorter. Apart from the recognized cell autonomous role in tumor suppression, we  
284 propose that telomere shortening affects tumorigenesis in a non-cell autonomous manner. As  
285 an organism grows older, increasing numbers of cells with short telomeres modulate their  
286 surrounding environment creating a pro-inflammatory milieu that promotes tumorigenesis.

287 Using zebrafish embryo chimeras and cancer transplants, we show that incidence of  
288 melanoma is not only higher but progresses faster in animals deficient for telomerase. Both  
289 adult G1 *tert*-/- and G2 *tert*-/- embryos have shorter telomeres and mount DNA damage  
290 responses that stabilize p53 leading to premature aging and death (13, 28, 29). Indeed,  
291 mutations in *tp53* rescue the severity of both *tert*-/- models, allowing for prolonged survival.  
292 Spontaneous cancer in zebrafish, as in humans, is an age-associated disease that quickly rises  
293 upon decline of reproductive age (13, 36). Like other age-related phenotypes, spontaneous  
294 tumors in *tert*-/- zebrafish are accelerated to younger ages, while remaining similar in  
295 incidence and spectrum. Indeed, telomerase deficiency and telomere shortening in zebrafish  
296 do not appear to restrain tumorigenesis. Rather, they promote early cancer incidence denoting  
297 a systemic role in their effects. Similarly, humans with deficiencies in telomerase and  
298 premature telomere shortening show an increased cancer predisposition at younger ages (12).  
299 Thus, beyond preventing uncontrolled cell proliferation, absence of telomerase and telomere

300 shortening appear to have a systemic role impairing health status and resistance to disease.

301 How could telomere shortening in surrounding tissues lead to increased incidence of  
302 cancer? We observed that *tert*-/- zebrafish present high levels of senescence. Studies *in vitro*  
303 revealed that senescent cells secrete SASP, composed by several inflammatory factors (14,  
304 15). In agreement, we observed that *tert*-/- zebrafish present high levels of *cdkn1a* and *ink4ab*  
305 senescence genes and TNF- $\alpha$ , a cytokine involved in systemic inflammation. Moreover, G2  
306 *tert*-/- cells are capable of inducing systemic senescence and inflammation in a non-cell  
307 autonomous manner. This data constitutes a strong indication that cells with short telomeres  
308 are a source of paracrine SASP *in vivo*. However, similar to other studies in zebrafish (37),  
309 we were unable to detect other typical SASP cytokines in *tert*-/- zebrafish larvae, such as IL6  
310 and IL10. The main *in vivo* SASP molecules are yet to be identified in zebrafish.

311 Consistent with higher levels of inflammatory cytokines, G2 *tert*-/- cells containing  
312 critically short telomeres can modulate their environment by increasing the number of  
313 neutrophils. An increase in innate immune cells is characteristic of an inflammatory  
314 environment which can be tumorigenic. Human skin cancers have been shown to increase  
315 upon repeated injury and ulcers of previous lesions (38). In zebrafish, Feng *et al.* showed that  
316 preventing the recruitment of innate immune cells reduced the growth of HRAS<sup>G12V</sup>-  
317 transformed cells (16). Moreover, PGE2 produced by immune cells were shown to constitute  
318 a source of supportive signals for cancer cell growth. In line with this study, we observed a  
319 reduction of melanoma invasiveness with anti-inflammatory treatment, such as Aspirin and  
320 Celecoxib. Thus, our results suggest that G2 *tert*-/- cells with short telomeres promote the  
321 tumor invasiveness through the COX-2 pathway.

322 Collectively, our data indicates that an environment with short telomeres promotes  
323 tumorigenesis in a non-cell autonomous manner and increases the invasiveness capacity of  
324 melanoma cells. Apart from the recognized cell autonomous role in blocking uncontrolled

325 cell division, telomere shortening and senescence may have a second, perhaps, antagonistic  
326 pleiotropic consequence of causing local tissue damage and chronic inflammation. Thus, we  
327 propose that telomere shortening during aging gives rise to a systemic inflammatory  
328 environment. Chronic inflammation may be part of the mechanism whereby telomere  
329 shortening leads to increase tumorigenesis with age. Indeed, whereas chronic inflammation  
330 was shown to be a contributing factor in several cancers, immunosuppression leads to  
331 increase the risk for certain tumors (39, 40). Epidemiology studies associate the long-term  
332 dosage of Aspirin with a reduced incidence of certain types of cancer (18–20). Interestingly,  
333 this effect is more pronounced with increased age of the population. Reverting telomere  
334 shortening in animal models that possess short telomeres, such as the zebrafish, will  
335 conclusively test the idea if repression of telomerase promotes cancer in aging.

336

337

338 **Materials and Methods**

339 **Ethics statement**

340 All Zebrafish work was conducted according to National Guidelines and approved by the  
341 Ethical Committee of the Instituto Gulbenkian de Ciência and the DGAV (Direcção Geral de  
342 Alimentação e Veterinária, Portuguese Veterinary Authority).

343 **Zebrafish maintenance and standard techniques**

344 Zebrafish were maintained in accordance with Institutional and National animal care  
345 protocols. For normal line maintenance embryos were collected from crosses and kept in E3  
346 embryo medium (5.0mM NaCl, 0.17mM KCl, 0.33mM CaCl, 0.33mM MgSO<sub>4</sub>, 0.05%  
347 methylene blue, pH 7.4) at 28°C on a 14h light/10h dark cycle. At 5-6dpf larvae were  
348 transferred into a recirculating system at 28°C, with a 14h light/10h dark cycle.  
349 For anesthesia, fish were immersed into tricaine methane sulfonate solution at 168µg/L

350 (MS222 Sigma) and after the procedure placed back into system water. Their recovery was  
351 monitored until they regained normal swimming ability. Tricaine methane sulfonate was used  
352 at high concentration (200mg/L) to sacrifice fish. Larvae (until 7dpf) were sacrificed by  
353 placing them in ice-cold water for longer than 20min.

354 **Transgenic and mutant zebrafish lines**

355 The telomerase mutant line *tert*<sup>AB/hu3430</sup> generated by N-Ethyl-Nnitrosourea (ENU)  
356 mutagenesis (Utrecht University, Netherlands; Wienholds, 2004), has a T→A point-mutation  
357 in the *tert* gene and is available at the ZFIN repository, ZFIN ID: ZDB-GENO-100412-50,  
358 from the Zebrafish International Re-source Center – ZIRC. The *tert*<sup>hu3430</sup> mutation was  
359 combined by genetic crossing in a *casper* background strain leading to the complete lack of  
360 pigmentation (41). For maintenance of this line, *casper*; *tert*<sup>AB/hu3430</sup> was continuously  
361 outcrossed to *casper*; *tert*<sup>+/+</sup>. All recipient embryos used for the generation of HRAS  
362 chimeras, *tert*<sup>hu3430/hu3430</sup> homozygous mutants (referred to as *tert*-/-) as well as their WT  
363 siblings were obtained by incrossing *casper*; *tert*<sup>AB/hu3430</sup> animals. Donor embryos carry two  
364 different transgenes: Tg(*mitfa:HRAS*<sup>G12</sup>-*mitfa:GFP*;  $\beta$ -actin:*mGFP*). They express GFP and  
365 a mutated and oncogenic version of human HRAS under a melanocyte-specific promoter  
366 *mitfa* causing strong hyperpigmentation and the formation of melanoma (23). We used a  
367 Tg( $\beta$ -actin:*mGFP*) line with ubiquitous expression of membrane bound-GFP (mGFP) (42),  
368 since *mitfa:GFP* is only visible upon melanocyte development.

369 **Generation of zebrafish chimeras**

370 Both donor and recipient embryos were manually dechorionated using forceps (not earlier  
371 than 16 cell-stage). Dechorionated embryos were maintained in transplant-media (14.97mM  
372 NaCl; 503μM KCl; 1.29mM CaCl<sub>2</sub> · 2H<sub>2</sub>O; 150.63μM KH<sub>2</sub>PO<sub>4</sub>; 50μM Na<sub>2</sub>HPO<sub>4</sub>;  
373 994.04μM MgSO<sub>4</sub> · 7H<sub>2</sub>O) with penicillin/streptomycin (100U/ml penicillin and 100μg/ml  
374 streptomycin) in agarose-coated plates until 48hpf after which they were transferred into E3

375 embryo medium in non-coated petri dishes. Cell transfer from donor to recipient embryo was  
376 performed at blastula-stage using a hydraulic, manual microinjector (CellTram® vario,  
377 Eppendorf) with needles pulled from capillaries (TW100-4, World precision instruments,  
378 with a tip clipped off and polished of inner diameter at the tip 40-45 $\mu$ m) using a fluorescent  
379 stereoscope (Leica M205FA). Labelled donor cells (GFP+) were taken from  
380 Tg(*mitfa:HRAS*<sup>G12</sup>-*mitfa:GFP*;  $\beta$ -actin:*mGFP*) embryos and injected into recipient embryos.  
381 Cells were taken up by gentle suction directly at the blastula surface and released by injecting  
382 into the blastula of the recipient without ever harming the yolk cell. To increase the  
383 likelihood of transferring neural crest progenitors for tumor studies in adult animals, cells  
384 were typically taken from 3-5 spots at different sides of the donor embryo, all aligned  
385 midway between animal pole and yolk cell. Directly upon transfer, around 5% (estimation) of  
386 cells in a chimeric embryo were donor-derived. Single donor embryos served usually for  
387 various recipients (up to four), but one recipient never received cells from mixed donors.  
388 Upon cell transfer embryos were kept at low density (max 50 per plate) at 28°C and cleaned  
389 daily.

### 390 **Selection of Chimeras to grow and tumor assessment**

391 All animals included in this study were screened for a normal phenotype, presence of  
392 melanocytes and presence of GFP-positive donor cells. This screening was done under light  
393 anesthesia (84 $\mu$ g/L tricaine methane sulfonate MS222 in E3 embryo medium, 50% of  
394 standard concentration) under a Fluorescence stereomicroscope (Leica M205FA).  
395 Tumor appearance was assessed weekly and macroscopically. Individual animals were scored  
396 for the onset of a vertical growth phase, the presence of an outgrowth in any direction.  
397 Subsequently, most animals were analyzed by histopathology to confirm tumor formation and  
398 the state of invasiveness.

### 399 **Fish preservation for histology**

400 When possible, fish were food-deprived for 24h prior to processing. After sacrificing,  
401 pictures of each fish were taken from both sides, both with a regular camera and at the  
402 fluorescent stereoscope (Leica M205FA) to save information about the gross distribution of  
403 pigmentation and chimeric (GFP+) cells. Animals were fixed in 10% neutral buffered  
404 formalin for 72h at room temperature and decalcified in 0.5M EDTA for 48h. Whole fish  
405 were paraffin embedded and 3 $\mu$ m transversal cuts were done from 5-8 regions of the fish  
406 (depending on size). Cuts were stained with haematoxylin and eosin and analyzed by  
407 histopathology. A total of N=18 animals was analyzed (9 WT and 9 *tert*-/- recipients).

408 **Melanoma cell transplants into 2dpf larvae**

409 Melanoma cells were derived from Tg(*mitfa:HRAS*<sup>G12</sup>-*mitfa:GFP*) zebrafish tumors. To  
410 obtain the tumor cells fish were first sacrificed with tricaine 25x and the tumor was dissected  
411 with a regular scalpel and scissors. To dissociate the tumor, the mass of cells was dissected in  
412 small pieces, placed in a tryplE solution and pipetted up and down. Enzymatic reaction was  
413 stop with the addition of FBS (10% of total volume). Solution was filtered (70 $\mu$ m filter) and  
414 spun down at 1700 rpm for 5 min. The pellet was re-suspended in PBS calcium/magnesium  
415 free and then washed in culture medium with PBS (DMEM + 10% FBS). The final solution  
416 was approximately 1x10<sup>7</sup> cells/mL and was obtained by removing as much as possible  
417 supernatant in the last centrifugation.

418 Melanoma cells were injected into the circulation of 2dpf larvae with a microinjection  
419 apparatus and needles were pulled from capillaries (TW100-4, World precision instruments).

420 Transplanted larvae were kept overnight at 28°C in embryo media. In the following day  
421 larvae are screened for the presence of GFP positive cells in the tail region and only those  
422 continue in the experiment. Pictures were taken at 1, 4 and 7 days-post injection using a  
423 fluorescent stereoscope (Leica M205FA). Transplanted larvae were kept in individual wells  
424 of a 6 well-plate to allow individual tracking of melanoma progression. Control (E3) or

425 treatment (Aspirin - 30 $\mu$ M; Celecoxib – 25 $\mu$ M dissolved in DMSO) media were replaced  
426 daily. These experiments were repeated 2-3 times. GFP area was quantified using the  
427 Analyze Particles tool of imageJ 1.52i software.

428 **Statistical analysis**

429 Statistical analysis was done with the Software GraphPad Prism 6. Comparisons of two  
430 different points were done by unpaired t-test. For the G1 HRAS chimeras, comparison over  
431 time (for at least 2 timepoints) was performed by Two-way RM ANOVA. Tumor onset over  
432 time was compared using a Log-rank (Mantel-Cox) test. A critical value for significance of  
433 p<0.05 was used throughout the study. For the larvae transplants, trend lines of GFP area  
434 between the three time-points (1, 4 and 7 days-post injection) per transplanted zebrafish were  
435 calculated using Microsoft Excel 2010 software. Slopes averages were compared between  
436 each two conditions using unpaired t-test with the Software GraphPad Prism 6.

437 **Senescence-associated  $\beta$ -galactosidase assay**

438  $\beta$ -galactosidase assay was performed as previously described (43). Briefly, sacrificed  
439 zebrafish larvae were fixed over-night in 4% paraformaldehyde in PBS at 4°C and then  
440 washed three times for 1 h in PBS-pH 7.4 and for a further 1 h in PBS-pH 6.0 at 4°C.  $\beta$ -  
441 galactosidase staining was performed for 10h at 37°C in 5 mM potassium ferrocyanide, 5  
442 mM potassium ferricyanide, 2mM MgCl<sub>2</sub> and 1 mg/ml X-gal, in PBS adjusted to pH 6.0.  
443 After staining, larvae were washed three times for 5 minutes in PBS pH 7, observed and  
444 photographed using a bright filter stereoscope (Leica M205FA).

445 **Real-time quantitative PCR**

446 4dpf larvae were sacrificed, immediately snap-frozen in liquid nitrogen and collected in  
447 Eppendorf tube, minimum 10 larvae each. RNA extraction was performed using a RNeasy  
448 extraction kit (Qiagen, UK # 50974134). Briefly, larvae were smashed in RLT lysis buffer  
449 (provided by the kit) and the extract was washed and RNAs isolated through RNA binding

450 column and eluted in dH<sub>2</sub>O RNase-free, according to manufacture procedures. Quality of  
451 RNA samples was assessed through BioAnalyzer (Agilent 2100, CA, USA). Retro-  
452 transcription into cDNA was performed using a RT-PCR kit NZY First-Strand cDNA  
453 Synthesis Kit # MB12501 (NZYtech). Quantitative PCR (qPCR) was performed using iTaq  
454 Universal SYBR Green Supermix # 1725125 (Bio-Rad) and an ABI-QuantStudio 384  
455 Sequence Detection System (Applied Biosystems, CA, USA). qPCRs were carried out in  
456 triplicate for each cDNA sample. Relative mRNA expression was normalized to rpl13 mRNA  
457 expression using the DCT method. Primer sequences are listed in Table S1.

458  
459 **Table S1 – List of primers used in RT-qPCR expression analysis and *tert* genotyping.**

Gene name	Primer sequences
<i>p15/16</i>	forward – 5' GGATGAAGTGACCACAGCAGCA 3' reverse – 5' CGGCTGCGGAAAGAGTCTCAG 3'
<i>p21</i>	forward – 5' ATGCAGCTCCAGACAGATGA 3' reverse – 5' CGCAAACAGACCAACATCAC 3'
<i>TNF<math>\alpha</math></i>	forward – 5' AGGCAATTCACTTCCAAGGC 3' reverse – 5' GGTCTGGTCATCTCTCCAGT 3'
<i>RPL13</i>	forward – 5' TTCACCACACAGCCGAAAGA 3' reverse – 5' TACCGCAAGATTCCATACCCA 3'

460

## 461 **Acknowledgements**

462 We thank members of the Telomeres and Genome Stability Laboratory for helpful  
463 discussions. We are grateful to Yi Feng (U of Edinburgh), Thiago Carvalho (Fundação  
464 Champalimaud) and Leonor Saúde (Instituto de Medicina Molecular) for critically reading  
465 our manuscript. We thank the Instituto Gulbenkian de Ciência histology unit and the Fish

466 Facility for excellent animal care. KL was a recipient of a Portuguese Fundacão para a  
467 Ciéncia e a Tecnologia (FCT) fellowship SFRH/BD/52173/2013. This work was supported  
468 by the FCT (PTDC/BIM-ONC/3402/2014 and PTDC/SAU-ONC/116821/2010) and the  
469 Howard Hughes Medical Institute grants received by MGF.  
470

471 **Author contributions**

472 Conceived and designed the experiments: MGF KL MF and MMG. Performed the  
473 experiments: KL MMG MF MM BLB KG. Analysed the data: KL MMG MF TC MGF.  
474 Contributed reagents/materials/analysis tools: KL MMG MF MM BLB KG TC MGF. Wrote  
475 the paper: MGF KL MMG.  
476

477 **References**

- 478 1. Parkin DM, Pisani P, Ferlay J (1999) Global cancer statistics. *CA Cancer J Clin* 49(1):33–64.
- 479 2. Aubert G, Lansdorp PM (2008) Telomeres and Aging. *Physiol Rev* 88(2):557–579.
- 480 3. Palm W, de Lange T (2008) How shelterin protects mammalian telomeres. *Annu Rev Genet* 42:301–334.
- 481 4. Samassekou O, Gadji M, Drouin R, Yan J (2010) Sizing the ends: Normal length of  
482 human telomeres. *Ann Anat - Anat Anzeiger* 192(5):284–291.
- 483 5. Zhang X, Mar V, Zhou W, Harrington LA, Robinson MO (1999) Telomere shortening  
484 and apoptosis in telomerase-inhibited human tumor cells. *Genes & Dev* 13(18):2388–2399.
- 485 6. Fagagna F d'Adda di, et al. (2003) A DNA damage checkpoint response in telomere-  
486 initiated senescence. *Nature* 426(6963):194–198.
- 487 7. Lechel A, et al. (2005) The cellular level of telomere dysfunction determines induction  
488 of senescence or apoptosis in vivo. *EMBO Rep* 6(3):275–281.
- 489 8. Harley C (2008) Telomerase and cancer therapeutics. *Nat Rev Cancer* 8(3):167–179.
- 490 9. Shay JW, Wright WE (2011) Role of telomeres and telomerase in cancer. *Semin  
491 Cancer Biol* 21(6):349–353.
- 492 10. Armanios M, Blackburn EH (2012) The telomere syndromes. *Nat Rev Genet*  
493 13(10):693–704.
- 494 11. Holohan B, Wright WE, Shay JW (2014) Telomeropathies: An emerging spectrum  
495 disorder. *J Cell Biol* 205(3):289–299.
- 496 12. Alter BP, Giri N, Savage SA, Rosenberg PS (2009) Cancer in dyskeratosis congenita.  
497 *Blood*. doi:10.1182/blood-2008-12-192880.
- 498 13. Carneiro MC, et al. (2016) Short Telomeres in Key Tissues Initiate Local and

502        14. Systemic Aging in Zebrafish. *PLOS Genet* 12(1):e1005798.

503        14. Coppé J-P, et al. (2008) Senescence-Associated Secretory Phenotypes Reveal Cell-  
504        Nonautonomous Functions of Oncogenic RAS and the p53 Tumor Suppressor. *PLoS Biol* 6(12):e301.

505        15. Coppé J-P, Desprez P-Y, Krtolica A, Campisi J (2010) The Senescence-Associated  
506        Secretory Phenotype: The Dark Side of Tumor Suppression. *Annu Rev Pathol Mech  
507        Dis.* doi:10.1146/annurev-pathol-121808-102144.

508        16. Feng Y, Renshaw S, Martin P (2012) Live Imaging of Tumor Initiation in Zebrafish  
509        Larvae Reveals a Trophic Role for Leukocyte-Derived PGE2. *Curr Biol* 22(13):1253–  
510        1259.

511        17. Feng Y, Martin P (2015) Imaging innate immune responses at tumour initiation: New  
512        insights from fish and flies. *Nat Rev Cancer.* doi:10.1038/nrc3979.

513        18. Cao Y, et al. (2016) Population-wide Impact of Long-term Use of Aspirin and the Risk  
514        for Cancer. *JAMA Oncol* 2(6):762.

515        19. Gamba CA, et al. (2013) Aspirin is associated with lower melanoma risk among  
516        postmenopausal Caucasian women: The Women's Health Initiative. *Cancer.*  
517        doi:10.1002/cncr.27817.

518        20. Rothwell PM, et al. (2011) Effect of daily aspirin on long-term risk of death due to  
519        cancer: analysis of individual patient data from randomised trials. *Lancet*  
520        377(9759):31–41.

521        21. Kim IS, et al. (2017) Microenvironment-derived factors driving metastatic plasticity in  
522        melanoma. *Nat Commun* 8(1):14343.

523        22. Tobia C, Gariano G, De Sena G, Presta M (2013) Zebrafish embryo as a tool to study  
524        tumor/endothelial cell cross-talk. *Biochim Biophys Acta - Mol Basis Dis.*  
525        doi:10.1016/j.bbadic.2013.01.016.

526        23. Michailidou C, et al. (2009) Dissecting the roles of Raf- and PI3K-signalling pathways  
527        in melanoma formation and progression in a zebrafish model. *Dis Model & Mech*  
528        2(7–8):399–411.

529        24. Henriques CM, Carneiro MC, Tenente IM, Jacinto A, Ferreira MG (2013) Telomerase  
530        is required for zebrafish lifespan. *PLoS Genet* 9(1):e1003214.

531        25. AI B, C C (2007) TUMOR CELL MORPHOLOGY. *Comparative Oncology.*

532        26. Fior R, et al. (2017) Single-cell functional and chemosensitive profiling of  
533        combinatorial colorectal therapy in zebrafish xenografts. *Proc Natl Acad Sci U S A*  
534        114(39). doi:10.1073/pnas.1618389114.

535        27. Moore JC, Langenau DM (2016) Allograft Cancer Cell Transplantation in Zebrafish.  
536        *Advances in Experimental Medicine and Biology*, pp 265–287.

537        28. Anchelin M, et al. (2013) Premature aging in telomerase-deficient zebrafish. *Dis  
538        Model & Mech* 6(5):1101–1112.

539        29. Henriques CM, Carneiro MC, Tenente IM, Jacinto A, Ferreira MG (2013) Telomerase  
540        Is Required for Zebrafish Lifespan. *PLoS Genet* 9(1).  
541        doi:10.1371/journal.pgen.1003214.

542        30. Harley C, et al. (1992) Telomere length predicts replicative capacity of human  
543        fibroblasts. *Proc Natl Acad Sci U S A* 89(21):10114–10118.

544        31. Renshaw SA, et al. (2006) A transgenic zebrafish model of neutrophilic inflammation.  
545        *Blood* 108(13):3976–3978.

546        32. Ostrand-Rosenberg S (2008) Immune surveillance: a balance between protumor and  
547        antitumor immunity. *Curr Opin Genet Dev.* doi:10.1016/j.gde.2007.12.007.

548        33. Loynes CA, et al. (2018) PGE2 production at sites of tissue injury promotes an anti-  
549        inflammatory neutrophil phenotype and determines the outcome of inflammation  
550        resolution in vivo. *Sci Adv.* doi:10.1126/sciadv.aar8320.

551

552 34. Freisinger CM, Huttenlocher A (2014) Live imaging and gene expression analysis in  
553 zebrafish identifies a link between neutrophils and epithelial to mesenchymal  
554 transition. *PLoS One*. doi:10.1371/journal.pone.0112183.

555 35. Heidenreich B, Rachakonda PS, Hemminki K, Kumar R (2014) TERT promoter  
556 mutations in cancer development. *Curr Opin Genet Dev*.  
557 doi:10.1016/j.gde.2013.11.005.

558 36. Feitsma H, Cuppen E (2008) Zebrafish as a cancer model. *Mol Cancer Res*.  
559 doi:10.1158/1541-7786.MCR-07-2167.

560 37. Novoa B, et al. (2019) Rag1 immunodeficiency-induced early aging and senescence in  
561 zebrafish are dependent on chronic inflammation and oxidative stress. *Aging Cell*.  
562 doi:10.1111/ace.13020.

563 38. Maru GB, Gandhi K, Ramchandani A, Kumar G (2014) The Role of Inflammation in  
564 Skin Cancer. *Inflammation and Cancer* doi:10.1007/978-3-0348-0837-8.

565 39. Tang L, Wang K (2016) Chronic inflammation in skin malignancies. *J Mol Signal*.  
566 doi:10.5334/jmols.2016.070002.

567 40. Shalapour S, Karin M (2015) Immunity, inflammation, and cancer: An eternal fight  
568 between good and evil. *J Clin Invest*. doi:10.1172/JCI80007.

569 41. White RM, et al. (2008) Transparent Adult Zebrafish as a Tool for In Vivo  
570 Transplantation Analysis. *Cell Stem Cell*. doi:10.1016/j.stem.2007.11.002.

571 42. Cooper MS, et al. (2005) Visualizing morphogenesis in transgenic zebrafish embryos  
572 using BODIPY TR methyl ester dye as a vital counterstain for GFP. *Dev Dyn*.  
573 doi:10.1002/dvdy.20252.

574 43. Kishi S, et al. (2008) The identification of zebrafish mutants showing alterations in  
575 senescence-associated biomarkers. *PLoS Genet* 4(8).  
576 doi:10.1371/journal.pgen.1000152.

577 578

## 579 **Figure Legends**

580 **Figure 1. Short telomeres promote tumorigenesis in a non-cell autonomous manner. A)**  
581 Experimental setup for the generation of zebrafish chimeras. Donor cells are transplanted  
582 from a Tg(*mitfa:HRAS*<sup>G12V</sup>;  $\beta$ -actin:GFP) embryo at the blastula stage into embryos resulting  
583 from an incross of *tert*+/-. Casper zebrafish. B) Representative images of adult chimera  
584 zebrafish harboring melanoma in either WT or *tert*/- recipients. C) Melanoma occurrence  
585 over time in chimeric fish. *tert*/- recipient fish have a higher risk of tumorigenesis than WT  
586 recipient fish (p<0.05).

587 **Figure 2. *tert*/- tissues increase melanoma invasiveness and progression. A)** H&E images  
588 of melanoma arising in a wildtype (upper panel) or *tert*/- recipient fish. Strong infiltration  
589 into other tissues was typical in *tert*/- fish but not in wildtype (arrowheads). B) Melanoma

590 were staged according to histopathology into benign lesions (melanosis), non-invasive and  
591 invasive malignant tumors. C) Analysis of malignant tumors for cellular atypia. Sample  
592 numbers are indicated within the bars.

593 **Figure 3. G2 *tert*-/- larvae with very short telomeres exhibit increased melanoma  
594 micrometastasis.** A) Experimental design for melanoma allotransplants in zebrafish larvae.  
595 Melanoma tumors were dissociated from *mitfa:HRAS*;  $\beta$ -actin:GFP zebrafish. HRAS  
596 melanoma cells were then injected into blood circulation of 2dpf zebrafish larvae. Larvae  
597 were kept in embryo medium for 7 days post injection (7dpi). B) Representative images of  
598 HRAS melanoma cells spread (green) in WT or G2 *tert*-/- larvae at 7dpi. C) Time-course of  
599 HRAS melanoma cells spread in a group of WT and G2 *tert*-/- larvae (p<0.01 at 7dpi, WT  
600 N=10 and G2 *tert*-/- N=11). D) Melanoma tumors are more invasive in G2 *tert*-/- larvae  
601 (p=0.0205, WT N=32 and G2 *tert*-/- N=31). A linear regression of three time-points (1, 4 and  
602 7 dpi) was used to calculate the slope of melanoma invasiveness. Each dot represents one  
603 larvae allotransplant.

604 **Figure 4. Telomerase deficient tissues present higher levels of senescence and  
605 inflammation and modulate their environment.** A, B, C) RT-qPCR analysis comparing the  
606 expression levels of *ink4ab* (p16/15), *cdkn2a* (p21) and *tnfa* (TNF) of 4dpf WT and G2 *tert*-/-  
607 larvae and 9month WT and *tert*-/- adult intestine tissue (\* p<0.05, \*\* p<0.01 N=30). D)  
608 Representative images of SA- $\beta$ -Gal assay comparing WT and G2 *tert*-/- 4dpf zebrafish  
609 embryos. Yolk sack staining is nonspecific. E) Scheme for generating chimeras in which G2  
610 *tert*-/- blastula cells are transplanted into WT embryos (G2 *tert*-/- $\rightarrow$ WT). SA- $\beta$ -Gal assay  
611 showing increased senescence in 4dpf WT embryos with injection of G2 *tert*-/- cells. F)  
612 Scheme of G2 chimeras generation where WT or G2 *tert*-/- blastula cells are transplanted into  
613 WT Tg(*mpx:GFP*) embryos carrying labelled neutrophils with green fluorescent protein:  
614 WT $\rightarrow$ WT Tg(*mpx:GFP*) vs. G2 *tert*-/- $\rightarrow$ WT Tg(*mpx:GFP*). Representative images of the

615 chimeras at 4dpf, neutrophils are represented at green; G) Quantification of neutrophils at  
616 4dpf. Non-injected Tg(*mpx:GFP*) were used as controls. Each data point represents one  
617 zebrafish (\*\* p<0.01, non-injected N=24, WT N=33 and TERT N=25).

618 **Figure 5. Increased tumor invasiveness in G2 *tert*-/- larvae is rescued by inhibiting**  
619 **inflammation.** A) Allotransplants of primary tumor cells extracted from melanoma in adult  
620 fish into 2dpf larvae that were kept in embryo medium containing Aspirin or Celecoxib  
621 (COX-2 selective inhibitor). B) Representative images of melanoma invasiveness at 7dpi  
622 upon Aspirin treatment. C) Time-course of melanoma invasiveness in WT and G2 *tert*-/-  
623 larvae under Aspirin treatment. D) Slope of HRAS melanoma spread between 1, 4 and 7dpi.  
624 Comparison of invasiveness in a WT or G2 *tert*-/- either untreated (Control) or containing  
625 Aspirin (WT N=26 and G2 *tert*-/- N=29) or Celecoxib (WT N=19 and G2 *tert*-/- N=13). Each  
626 dot represents one zebrafish larva from 2-3 biological replicates.

627 **Supplementary Figure 1. *tert* genetic status of chimera recipients does not influence the**  
628 **number of melanocytes in larvae or adults.** A) Representative images of 3dpf chimeras  
629 exhibiting high (left) and low (right) number of melanocytes. Blastula mitfa:HRAS;  $\beta$ -  
630 actin:GFP cells were injected into the same stage embryos resulting from an incross of *tert*+/+  
631 ; Casper. Larvae were genotyped at 3dpf and followed individually until 11dpf. B) No  
632 significant differences can be observed between the number of melanocytes in hosts of  
633 different *tert* genotype, both at 3dpf and 11dpf. Each point in the graph represents an  
634 individual animal. Data are represented as mean +/- SEM. C) Chimeras harboring a tumor  
635 were analyzed for extent of pigmentation in adults. Left side animals with high pigmentation,  
636 right side: low pigmentation. C) Quantification of pigmented area given as in percent of total  
637 surface. Each datapoint represents one animal (both sides). Pigmented area did not  
638 significantly differ depending on the host genotype. Data are represented as mean +/- SEM.

639

Figure 1

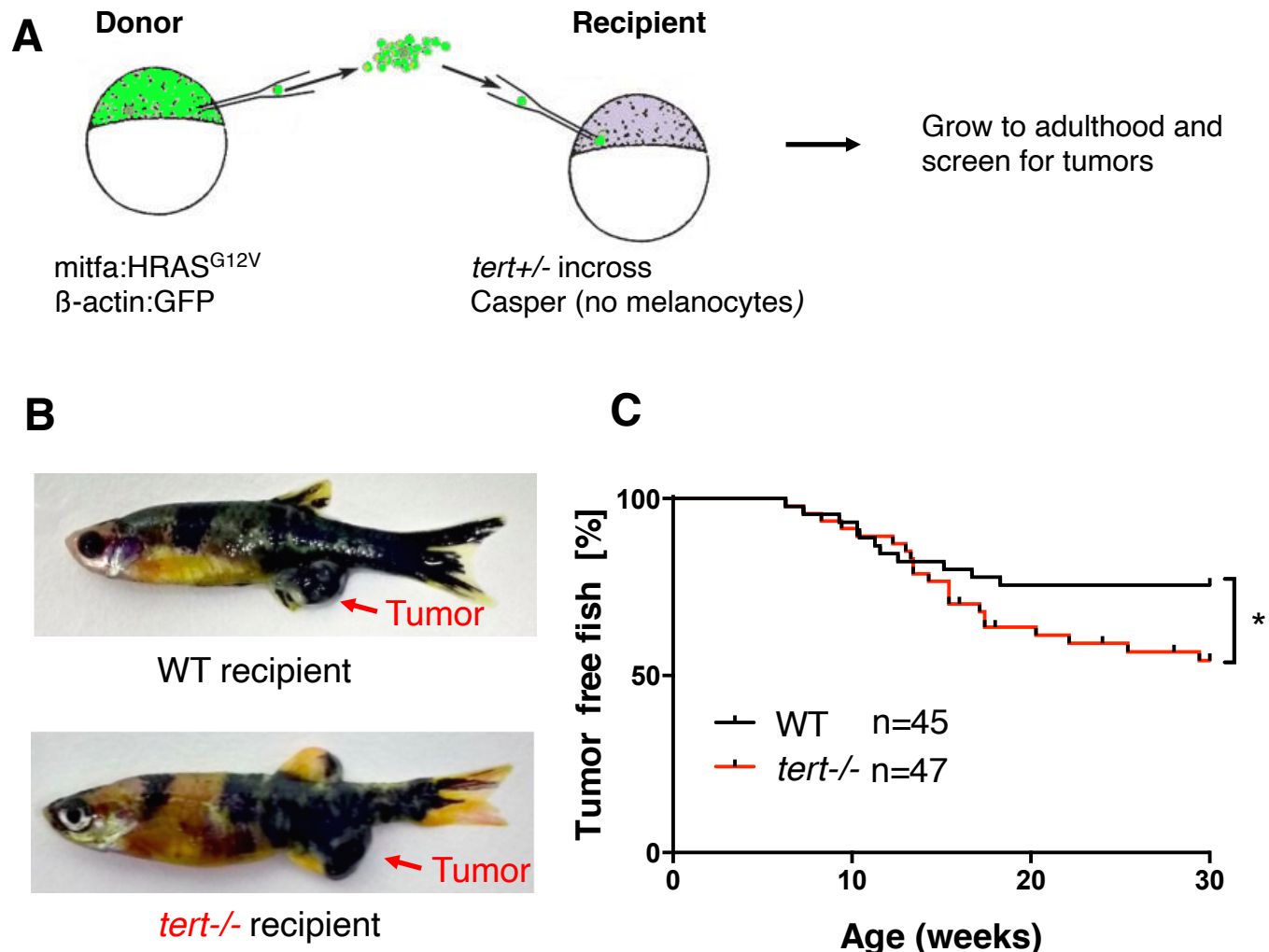
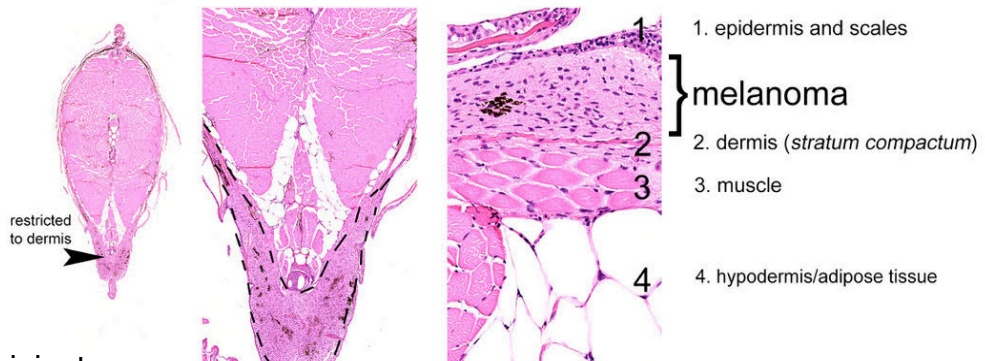


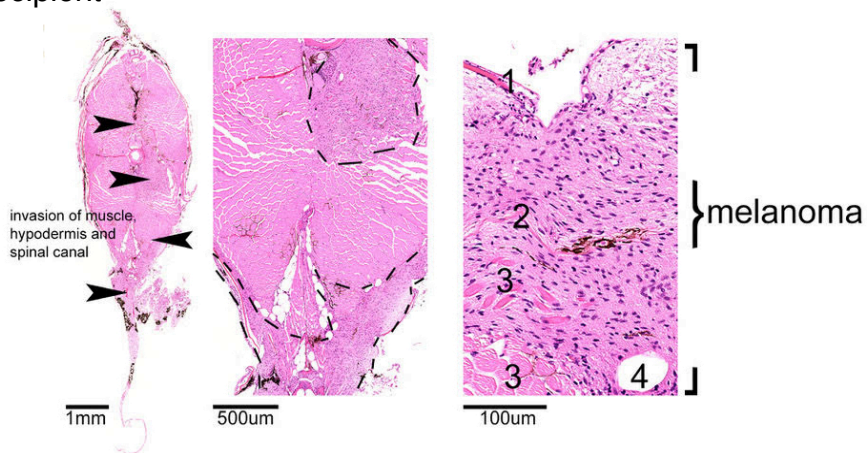
# Figure 2

**A**

WT recipient

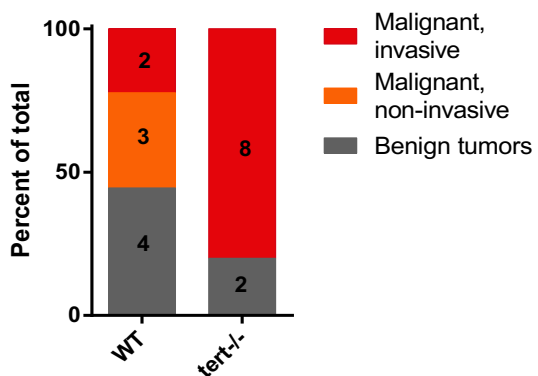


*tert*<sup>-/-</sup> recipient



**B**

Tumor staging



**C**

Cellular atypia

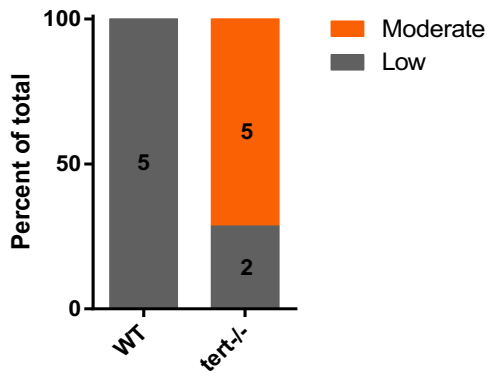
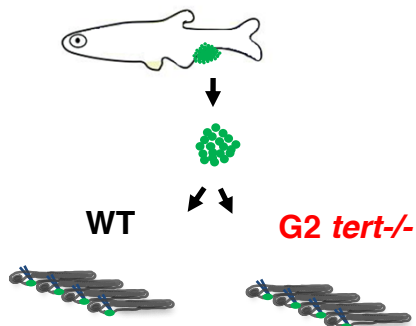
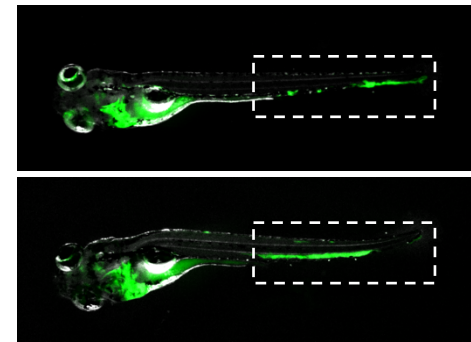


Figure 3

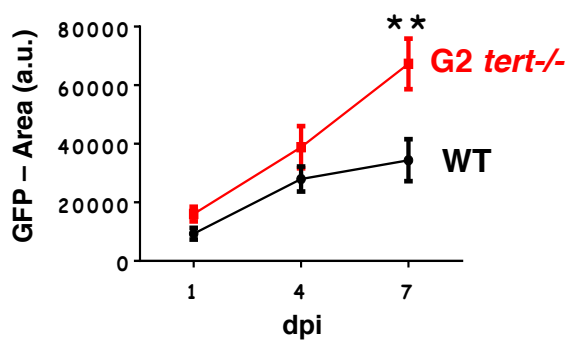
A



B



C



D

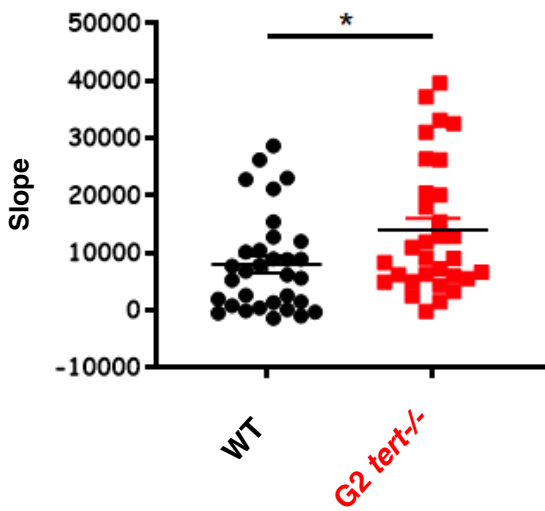


# Figure 4

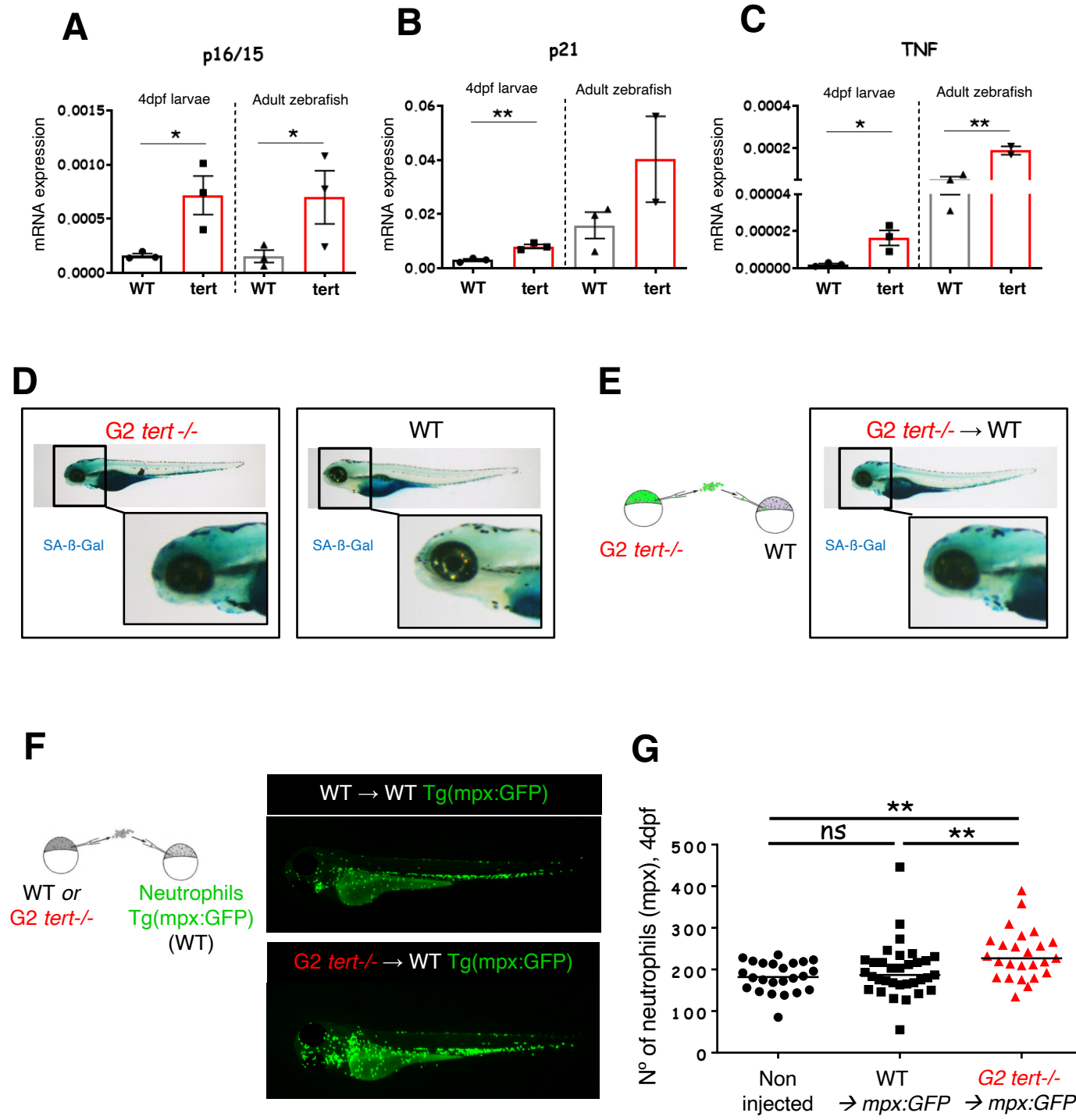
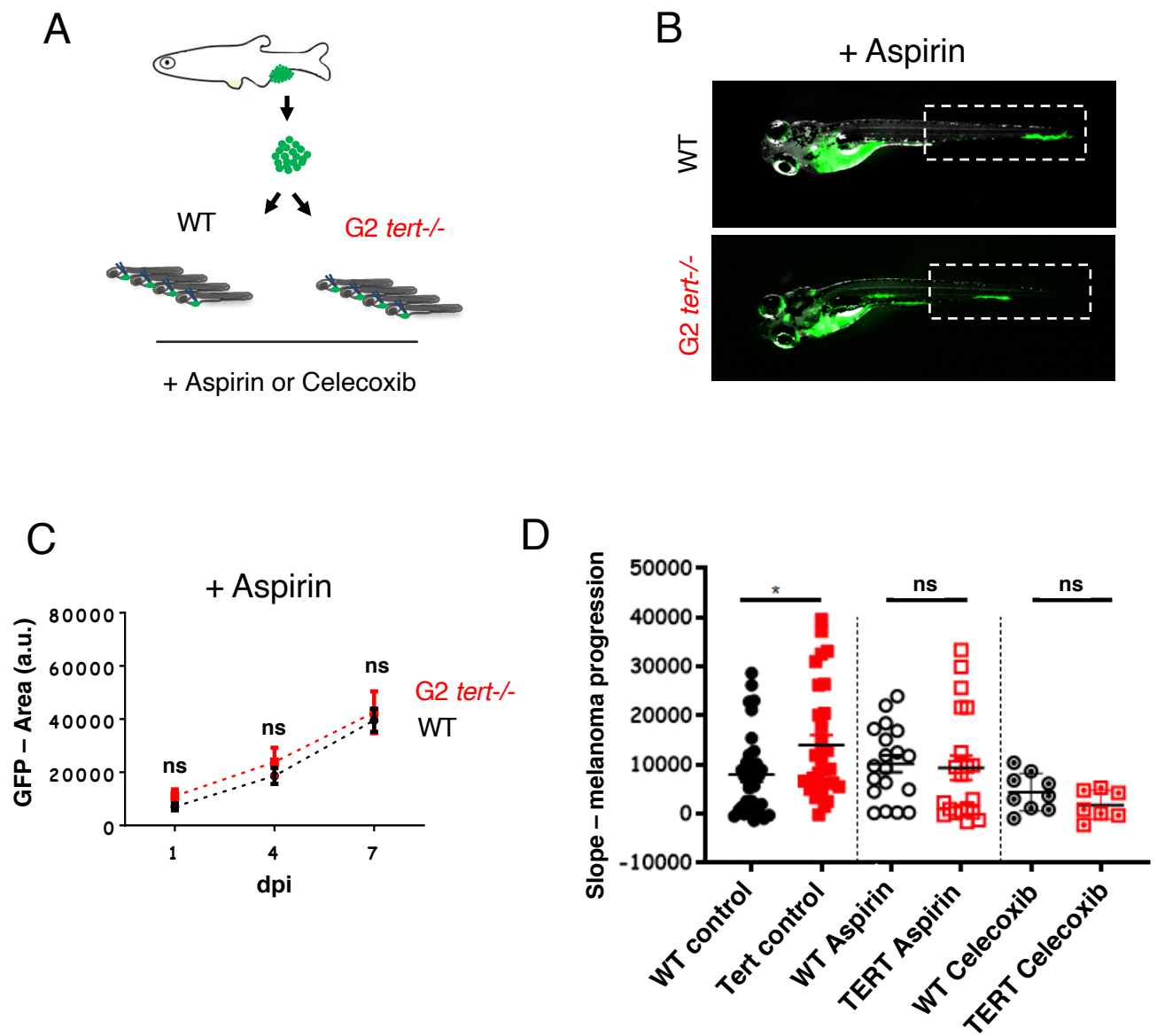
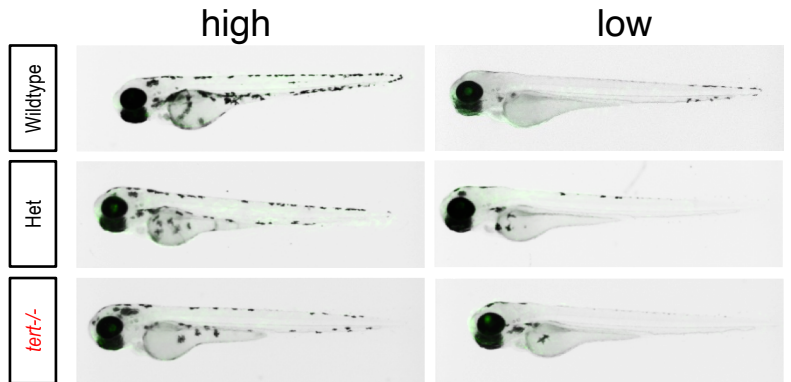


Figure 5



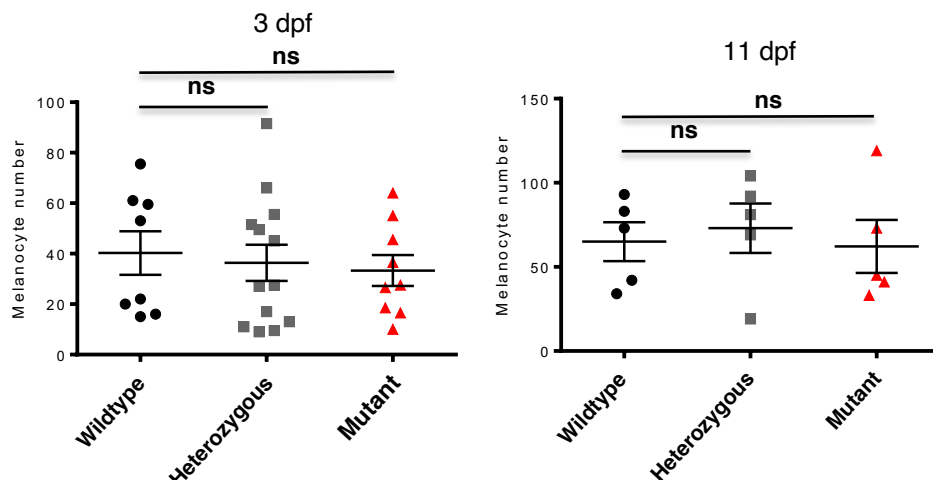
# Supplementary Figure 1

**A**

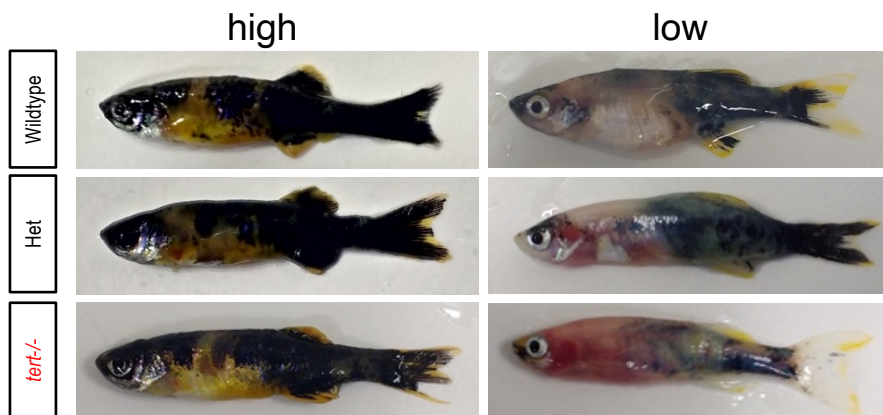


3 dpf

**B**



**C**



Adult

**D**

